Microchemical Journal 110 (2013) 146–157

Contents lists available at ScienceDirect

Microchemical Journal

journal homepage: www.elsevier.com/locate/microc

Investigations into the polymorphic properties of *N*,*N*-dimethyltryptamine by X-ray diffraction and differential scanning calorimetry

Alain Gaujac [a,b,c], James L. Ford [b], Nicola M. Dempster [b], Jailson Bittencourt de Andrade [a,d], Simon D. Brandt [b,*]

[a] Universidade Federal da Bahia, Campus Universitário de Ondina, 40170-115 Salvador-Ba, Brazil
[b] Liverpool John Moores University, School of Pharmacy and Biomolecular Sciences, L3 3AF, Liverpool, United Kingdom
[c] Instituto Federal de Educação, Ciência e Tecnologia de Sergipe, Br 101, Km 96, 49100-000 São Cristóvão-Se, Brazil
[d] Instituto Nacional de Ciência e Tecnologia, Centro Interdisciplinar de Energia e Ambiente, Campus Universitário de Ondina, 40170-115 Salvador-Ba, Brazil

ARTICLE INFO

Article history:
Received 2 March 2013
Received in revised form 12 March 2013
Accepted 12 March 2013
Available online 20 March 2013

Keywords:
N,*N*-dimethyltryptamine
DMT
Melting points
Polymorphism
Crystals
Differential scanning calorimetry
X-ray diffraction

ABSTRACT

The powerful psychoactive features of *N*,*N*-dimethyltryptamine (DMT) have sparked the imagination of many research disciplines for several decades. One of the key chemical features associated with compound identity is the determination of melting points. The descriptions of both melting points and morphology associated with DMT free base have long been a source of interest and discussion, especially when considering that these values encountered in the scientific literature range dramatically between 38–40 °C and 73–74 °C, respectively. Such variations in reported melting points suggest that DMT may exist in two or more polymorphic forms and it was the aim of this study to examine the potential polymorphism of DMT via X-ray powder diffraction (XRPD) and differential scanning calorimetry (DSC), including fast scan DSC. DMT samples were prepared following extraction from *Mimosa tenuiflora* inner barks or by laboratory synthesis and then its crystals were recrystallized from solutions of the alkaloid using either hexane or acetonitrile. Irrespective of source, crystals originating from synthesis were predominantly white crystals obtained using crystallization from hexane, whereas yellow samples following recrystallization with acetonitrile. Irrespective of source or solvent, two polymorphs appeared to exist with melting points, determined by DSC, of 57 °C to 58 °C for Form I and 45 °C to 46 °C for Form II. Estimates for their enthalpies were 91.9 ± 2.4 J g^{-1} for Form I and 98.3 ± 2.8 J g^{-1} for Form II. Form II converted to Form I during DSC; conversion was thus prevented by fast scanning rates of 100 °C min^{-1}. A transition temperature (T_g) in the range −21 °C (2 °C min^{-1}) to −13 °C (100 °C min^{-1}) was determined depending on DSC scanning rate. Its closeness to the melting point indicates a tendency of Form II to convert to Form I on storage, a phenomenon that was also facilitated by grinding. This study indicates that the presence of differently colored DMT free base crystals obtained from recrystallization might also point towards the existence of polymorphs rather than just the presence of impurities.

1. Introduction

The widespread interest in *N*,*N*-dimethyltryptamine (DMT) stems from its powerful psychoactive properties observed in humans and, for this reason, is frequently referred to as a psychedelic/hallucinogenic substance [1,2]. It is therefore not surprising that investigations into its (psycho-)pharmacological profile have been long carried out in order to elucidate the mechanisms involved in the changes of thought, perception, mood and cognition brought about by this simple indole alkaloid [3–6]. Although the synthesis of DMT was reported in 1931 [7], first observations regarding its psychoactive properties started to surface in the literature in the 1950s [8].

The need for chemical and analytical investigations associated with DMT [9,10] arises from several areas of inquiry which include the presence of DMT and related derivatives in psychoactive beverages used for religious and recreational purposes [11,12], its abundant presence in the plant kingdom [13], and the long-standing interest in DMT and other *N*,*N*-dimethylated analogs as naturally-occurring substances in humans [14]. In addition, a forensic perspective develops from the fact that DMT is a controlled substance which makes it an attractive target for clandestine synthesis and impurity profiling studies [15–17]. A simple but important feature of each chemical entity is the determination of melting points. However, as far as the availability of these data on DMT is concerned it was interesting to notice that the melting points reported for DMT free base ranged dramatically, i.e. between 38–40 °C [18] and 73–74 °C [19], respectively.

Such variations in reported melting points suggest that DMT may exist in two or more polymorphic forms. Generally, multiple crystal forms with different solid state properties can exhibit differences in bioavailability of the active drug substance [20]. Resolution of these polymorphs can be made by a combination of experimental techniques, in

* Corresponding author. Tel.: +44 151 231 2184; fax: +44 151 231 2170.
E-mail address: s.brandt@ljmu.ac.uk (S.D. Brandt).

0026-265X/$ – see front matter © 2013 Elsevier B.V. All rights reserved.
http://dx.doi.org/10.1016/j.microc.2013.03.009

this case X-ray powder diffraction (XRPD) and differential scanning calorimetry (DSC) [21,22]. Fast Scan DSC, where scanning rates up to 500 °C min^{-1} have been used, is a recently developed sub-technique of DSC [23] which has been used in the assessment of polymorphs that convert during analysis at conventional heating rates. Examples of drugs thus studied included carbamazepine [24] and sulfathiazole [25].

XRPD is a powerful tool in identifying different crystal phases and the position of diffraction peaks and the d-spacings that they represent provide information about the location of lattice planes in the crystal structure [26]. Each peak measures a d-spacing that represents a family of lattice planes and shifts in peak position or small changes in XRPD patterns can identify different hydrates of the same compound or the presence of additional polymorphic forms [27]. The aim of this study was to examine further the potential polymorphism of DMT via XRPD and DSC, including fast scan DSC, in an attempt to resolve the discrepancies in the melting points described in the literature and to assess the potential of the drug to form amorphous or waxy solids. The present investigation follows on from a previous report on an optimized isolation of DMT as reference material from *Mimosa tenuiflora* inner barks [28].

2. Experimental

2.1. Chemicals and reagents

All chemicals and reagents used were from Aldrich (Dorset, UK) and were of analytical grade or equivalent. *N*,*N*-Dimethyltryptamine (DMT) free base samples were obtained both from organic synthesis and isolation from *M. tenuiflora* inner barks as reported previously [15,28].

2.2. Sample preparation procedures

DMT samples were obtained by recrystallization of the crude alkaloid in hexane. The free base substance was dissolved in hexane at 40 °C to give a concentration of 30 g L^{-1}. After cooling to room temperature, the solutions were placed in a freezer at −18 °C for two days. Following crystallization, the mother solution was subsequently removed by filtration from the precipitated material. The pure DMT was dried gently under a stream of nitrogen, and stored at 4 °C until analysis. The free base products were dissolved at room temperature using minimal amounts of either hexane or acetonitrile until further dissolution was not observable. The solvent of each solution was evaporated at room temperatures under a gentle stream of nitrogen, giving samples W1, W2, Y1 and Y2. DMT samples W1 and W2 were predominantly white crystals obtained using crystallization from hexane; whereas yellow DMT samples Y1 and Y2 were obtained following crystallization with acetonitrile. Samples W1 and Y1 were crystallized from DMT prepared by organic synthesis, while samples W2 and Y2 were from DMT isolated from the bark of *M. tenuiflora*. Crystals were used without further treatment for DSC and XRPD except where samples of the four products were ground to determine the effect of grinding on their physical nature. Grinding of DMT samples was undertaken manually using an agate mortar and pestle performed using two different grinding intensities; i) brief crush and light grind and ii) a sixty second, more intensive, grind.

2.3. Instrumentation and experimental

2.3.1. Differential scanning calorimetry (DSC)

A PerkinElmer DSC 8000 with Intracooler 2 cooling accessory and Pyris v. 10.1.0.0420 software were used (Seer Green, UK). The furnace temperature was calibrated using the Perkin Elmer supplied standard reference materials indium (m.p. = 156.60 °C) and zinc (m.p. = 419.47 °C). Enthalpies of transition were calibrated with indium with a heat of fusion $\Delta H_f = 28.45$ J g^{-1}.

The sample size used was around 2–4 mg accurately weighed in crimped, standard aluminum pans. All samples were cooled to −40 °C at 50 °C min^{-1}, held isothermally for 1 min before heating at 2, 10, 20, 50 or 100 °C min^{-1} to 70 °C at which the temperature set points were held isothermally for 1 min. The cool−reheat cycle was then repeated following cooling from 70 °C to −40 °C at 50 °C min^{-1}, and again, samples were held isothermally at this temperature before subsequent reheating to 70 °C using the same temperature heating rate described above. In addition, untreated samples (W1 and W2 only) were heated at 10 °C min^{-1} to 45 °C, held isothermally at this temperature for 20 min prior to cooling to 25 °C. Samples were then cooled to −40 °C at 50 °C min^{-1}, held isothermally for 1 min and re-scanned from −40 °C at 2 °C min^{-1} to 70 °C. Extrapolated onset temperatures were used as the melting point (m.p.) of the samples. Glass transition temperatures were calculated from the point on heat flow curves where the specific heat change was half of the change in the complete transition [21]. The DMT samples were also analyzed at the fast scan heating rate (100 °C min^{-1}) following grinding.

2.3.2. X-ray powder diffraction (XRPD)

XRPD patterns were collected using a Rigaku Miniflex X-ray diffractometer (Osaka, Japan) calibrated using a silica standard plate. The patterns were obtained using Cu Kα (1.54 Å) radiation, a voltage of 30 kV, and a current of 15 mA. Samples were prepared in 0.5 mm diameter zero background sample holders and analyzed between 3 and 60°2θ, with step increments of 0.02°2θ and scanning speed of 2°2θ min^{-1}.

3. Results and discussion

Previous work on the isolation of DMT from *M. tenuiflora* inner barks was guided by its history of use in humans [29,30] and the need for reference material used for analytical determinations [28]. The present study employed fast scan DSC and XRPD to the characterization of DMT free base and aimed to assess the potential of the drug to form polymorphs and/or amorphous or waxy solids. Published melting points of DMT free base and their morphological variations are summarized in Table 1. The wide range observed from these data, and the lack of more detailed investigations, led to the consideration of potential polymorphism. The lowest melting point encountered was described by Whitney et al. who, following its preparation, described it as a pale amorphous solid that melted at 38 °C–40 °C [18]. At the other end of the spectrum was the report provided by Fish et al. that noted a melting point of 47 °C–49 °C following its synthesis and recrystallization from hexane. Interestingly, the authors then mentioned a conversion of this sample to a form with a higher melting point (71 °C–73 °C), also by recrystallization from hexane, by seeding with an authentic sample with a melting point of 73 °C–74 °C, respectively. More details about this conversion, however, were not reported [19]. Another study on the isolation of DMT from *Acacia maidenii* F. Muell. provided another example of the conversion of melting point values by seeding. In this case, the first melting point obtained after recrystallization from hexane was 46 °C–47 °C, and when the solution was seeded with an authentic sample (56 °C–58.5 °C), the corresponding melting point reported then was 57.5 °C–58.5 °C instead [31].

Following the implementation of liquid–liquid extraction using 60 g of powdered inner bark of *M. tenuiflora*, 421.4 mg of crude alkaloids (0.7% yield) was obtained from a concentrated hexane layer at 4 °C [28]. The majority of crystal material was white in color but spots of yellow-colored crystals were also observed. In order to carry out a recrystallization from hexane the total amount of crude alkaloids was re-dissolved in 10 mL of warm hexane (45 °C) which led to the formation of two distinctly colored layers. During analytical characterization (data not shown) it was found that both layers

Table 1
Melting points reported in the literature for DMT free base.

Melting point [°C]	(Re)crystallization solvent[a]	Comment	Reference
38–40	–	Pale amorphous solid	Whitney et al. [18]
39–44	–	White solid	Grina et al. [32]
44	Petroleum ether	–	Rovelli and Vaughan [33]
44–45	–	–	Sintas and Vitale [34]
44.6–46.8[b]	–	–	Hochstein and Paradies [35]
45	Hexane	–	Julia et al. [36]
45.5–46.8	Methanol	–	Meckes-Lozoya et al. [38]
45.8–46.8	Xylene	Fine needle-shaped crystals	Gonçalves de Lima [29]
45–47	–	Yellowish crystals	Wisconsin Alumni Research Foundation et al. [39]
45–49	–	–	Hall et al. [40]
45–47	–	Colorless crystals	Häfelinger et al. [41]
45–47	Hexane	Crystalline/colorless	Wenkert and Kryger [42]
46	Ethanol/petroleum ether	Plates	Fleming and Woolias [43]
45	Petroleum ether	–	Culvenor et al. [37]
46–47[c]	Hexane	–	Fitzgerald and Sioumis [31]
47	–	–	Ghosal and Mukherjee [44]
47	–	Very fine ill-defined needles	Manske [7]
47	–	Off-white solid	Shulgin and Shulgin [2]
47–48	–	–	Heinzelman and Szmuszkovicz [45]
47–49[d]	Hexane	–	Fish et al. [19]
48–49	Hexane	Colorless prisms	Ueno et al. [46]
48.5–49	Petroleum ether	Colorless needles	Ueno et al. [46]
48–49	Ethyl acetate/petroleum ether	–	Bodendorf and Walk [47]
48–49	Hexane/ethyl acetate	–	Pachter et al. [48]
48–49	–	–	Boit [49]
49	Petroleum ether	Colorless prisms	Morimoto and Matsumoto [50]
49	Petroleum ether	Colorless prisms	Morimoto and Oshio [51]
49–50	–	White, pungent-smelling crystalline solid	Shulgin [52]
49–50	Diethyl ether/petroleum ether	Colorless needles	Hoshino and Shimodaira [53]
53.5–57.5	Hexane	–	Arthur et al. [54]
55.5	Hexane	White crystals	Gaujac et al. [28]
57	Hexane[d]	–	Poisson [55]
57	Hexane	–	Kan-Fan et al. [56]
57.5–58.5[c]	Hexane	–	Fitzgerald and Sioumis [31]
57–59	–	Crystalline solid	Shulgin and Shulgin [2]
58.2	–	Transparent acicular	Bergin et al. [57]
64	Hexane/ethyl acetate (80:20)	White crystals	Moura et al. [58]
65.5	–	Transparent colorless hexagonal prisms	Falkenberg [59]
67	Hexane	White crystals	Shulgin and Shulgin [2]
67–68	Hexane	–	Shulgin and Shulgin [2]
71–73[e]	Hexane	–	Fish et al. [19]

[a] In cases where (re)crystallization solvents were not explicitly mentioned, melting points were obtained from the solid free base following evaporation of a solvent during work-up or following distillation of the crude product.
[b] Melting obtained from a second distillation. The first distillation yielded an oil that crystallized with a melting point of 44 °C–46 °C.
[c] DMT free base, isolated by column chromatography, was crystallized from hexane and yielded a m.p. of 46 °C–47 °C. It was then reported that a solution seeded with an authentic sample of DMT (m.p. 58 °C–58.5 °C) gave a m.p. of 57.5 °C–58. °C which was not depressed on mixing.
[d] Crystallization in hexane followed by sublimation.
[e] Recrystallization from hexane resulted in a product that melted at 47 °C–49 °C. The authors stated that this material was then converted to a "higher melting form (71 °C–73 °C) by crystallization from hexane after seeding with an authentic specimen of m.p. 73 °C–74 °C". Further details were not provided.

contained DMT where the bottom layer (yellow in color and minor in abundance with regards to volume) represented an amorphous, high density, and viscous form of pure DMT. The top transparent layer consisted of DMT dissolved in hexane. The transparent layer was removed and stored at −18 °C which led to the formation of white DMT crystals (181.0 mg, 0.3% yield). Storage of the yellow layer in the fridge at 5 °C produced a yellow amorphous solid which was not investigated further.

The effect of heating rates on the DSC heating scans of W1, W2, Y1 and Y2 are shown in Figs. 1–4. It is clear from cursive examination of these figures *in toto* that, at various heating rates, two endotherms were apparent which would correspond to two polymorphic forms of DMT. Increase in scanning rate increases the apparent size of endotherms or exotherms since DSC measures heat flow as a function of time and makes more apparent any change in heat flow. The heat flow will increase with increase in heating rate [60]. Adapting conventionally used classification, the higher melting polymorph was deemed Form I whereas the lower melting polymorph was termed Form II. Again, the scans corresponding to reheats all displayed a glass transition indicating the ability of DMT to form an amorphous state. Tables 2 to 5 give the melting points and thermodynamic data of W1, W2, Y1 and Y2, respectively.

One of the advantages of fast scan DSC was that the fast rates prevent transformation of a sample during the heating process which provides a scan more representative of the original material [23]. Fig. 1 shows the DSC of sample W1 that was recrystallized using hexane from DMT prepared by organic synthesis. Taking DSC scans from sample W1 at 100 °C min^{-1} as a starting point (Fig. 1a), it can be seen that there were two melting endotherms present with onset temperatures of 47.5 °C and 58.3 °C for Form II and Form I, respectively. At 50 °C min^{-1} sample W1 (Fig. 1b) again displayed two endotherms, in this case with an exotherm positioned between them indicating that when Form II melted, some recrystallization occurred into Form I prior to the melting of Form I. As the heating rates were further decreased (Fig. 1c and d), this recrystallization became more obvious, and indeed at 2 °C min^{-1}, there was less evidence of the melting of Form II which indicated that conversion to Form I occurred during the scanning of the samples (Fig. 1e). Fast-Scan DSC allowed melting of the metastable polymorph to be separated from any subsequent recrystallization because the later event was moved to a

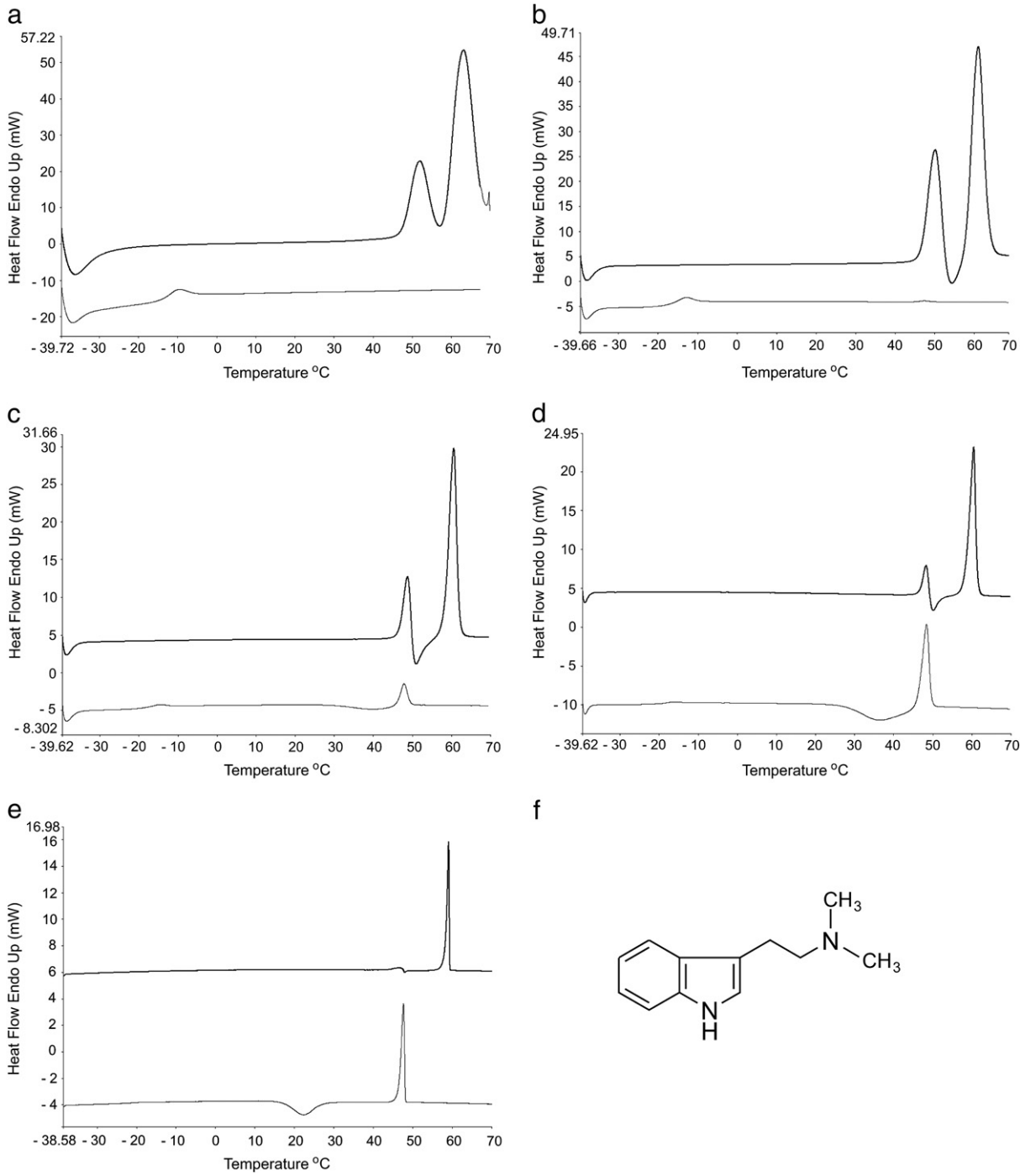

Fig. 1. DSC scans of sample W1 showing initial scan (upper) and re-scan (lower) curves obtained at a) 100 °C min^{-1} b) 50 °C min^{-1} c) 20 °C min^{-1} d) 10 °C min^{-1} and e) 2 °C min^{-1}; f) structure of *N*,*N*-dimethyltryptamine (DMT).

temperature higher than the melting temperature, i.e. providing separation of the events. Ford and Mann [23] demonstrated the use of Fast-Scan DSC in characterizing the polymorphic transitions of nifedipine. Using glassy material, the drug exhibited a number of transition events in the range 95 °C–110 °C at a heating rate of 10 °C min^{-1} and transitions from Form III to Form II and hence to Form I were easily observed. At higher scanning rates, the ratio of Form II to Form I changed during recrystallization and the relative amount of Form I increased with increase in scan rate (up to 300 °C min^{-1}) [23]. Further confirmation on the usefulness of Fast-Scan DSC was clearly demonstrated for carbamazepine which enabled the characterization of lower melting polymorphs by preventing multiple external events due to overlapping recrystallization [24].

In DMT sample W1, the general increase in the heat of fusion corresponding to Form II as the heating rate was increased (Table 2) further confirmed that the untreated sample contained both polymorphic forms. Assuming that 100% conversion to Form I occurred at 2 °C min^{-1}, an estimate for the enthalpy of fusion of Form I was made at 91.9 ± 2.4 J g^{-1}.

The re-scans show the glass transition temperatures (T_g) and are given in Table 2 with the 100 °C min^{-1} scan displaying only a glass transition and no subsequent recrystallization. The glass transition

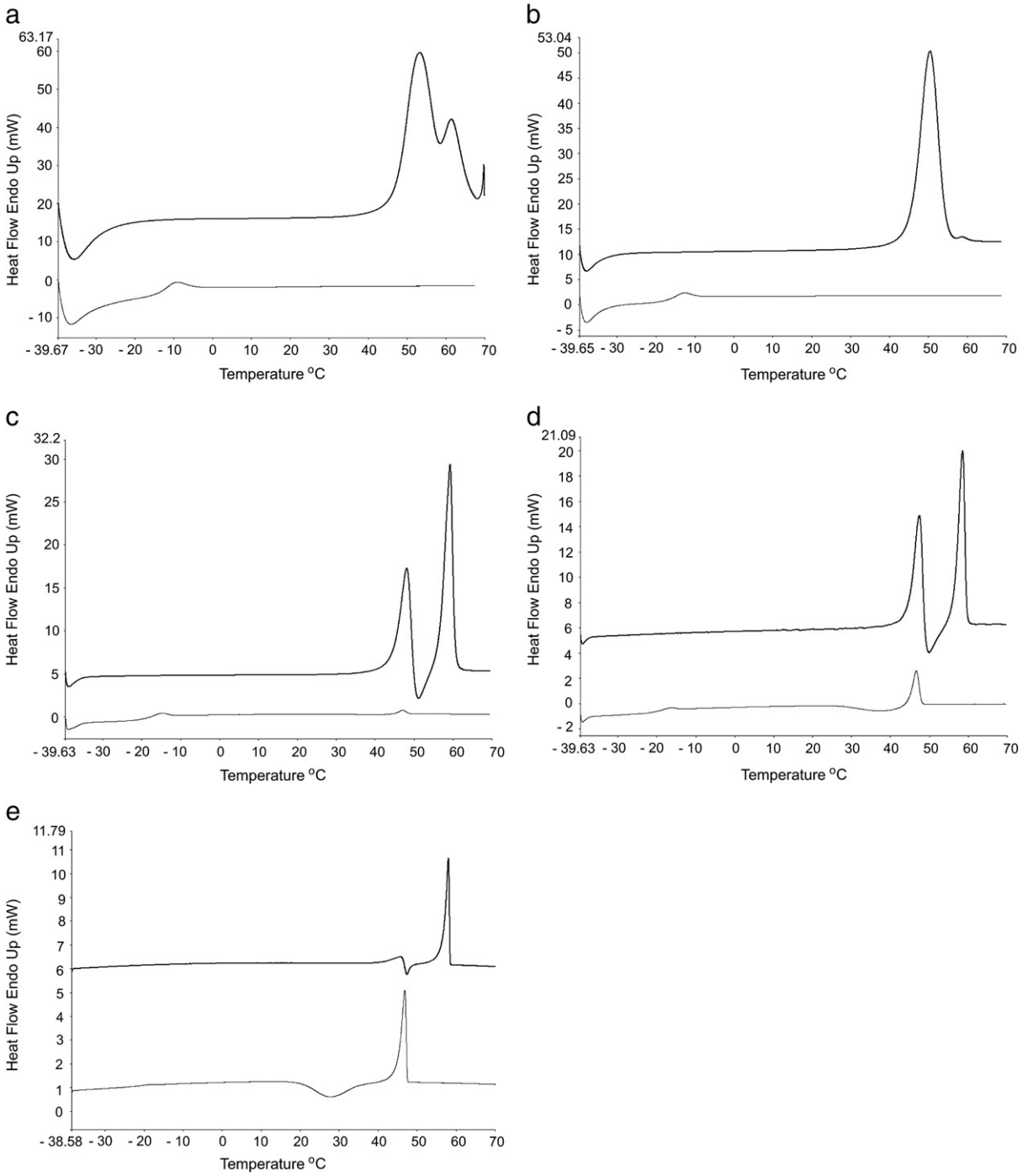

Fig. 2. DSC scans of sample W2 showing initial scan (upper) and re-scan (lower) curves obtained at a) 100 °C min^{-1} b) 50 °C min^{-1} c) 20 °C min^{-1} d) 10 °C min^{-1} and e) 2 °C min^{-1}.

represents the transformation from a glassy state to a rubbery state [61] and occurs at the T_g. Below this temperature the molecules are locked in position and relatively incapable of movement, whereas above the T_g, molecules are able to move and crystallization is favored. Decreasing heating rates showed an endotherm corresponding to the melting of Form II preceded by a recrystallization exotherm. This follows the expected thermodynamic theory that the less stable polymorph will crystallize from a melt on crystallization [62,63]. The recrystallization became more apparent as the heating rate decreased and concomitantly moved to lower temperatures. As expected the glass transition became less apparent with decreased scanning rates as the measured heat flow into and away from samples is reduced at lower scanning rates [23]. Assuming that the exotherm corresponded to 100% conversion to Form II, an enthalpy of fusion for this polymorph was estimated at 98.3 ± 2.8 J g^{-1}.

Fig. 2 shows the DSC of sample W2 that was recrystallized using hexane from the *M. tenuiflora* plant extract. Comparison of the scans obtained at 100 °C min^{-1}, (Figs. 2a and 1a) indicated that DMT W2 contained proportionately more of Form II. Indeed, at 50 °C min^{-1} the sample displayed almost exclusively the melting of Form II (Fig. 2b) but its enthalpy of fusion was 73.5 ± 0.5 J g^{-1} and indicated that there was some Form I in the sample. Scans at 20 °C, 10 °C and

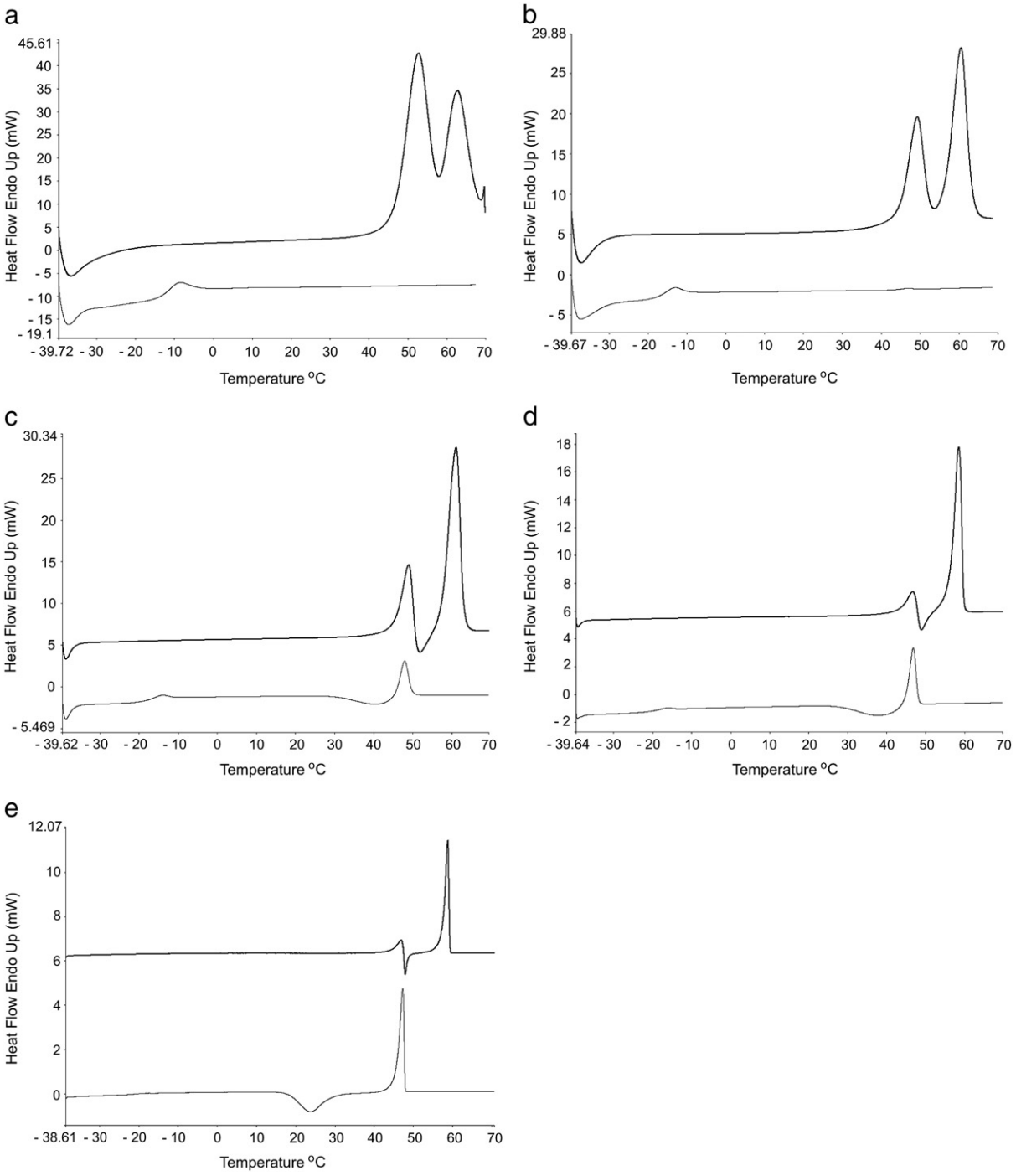

Fig. 3. DSC scans of sample Y1 showing initial scan (upper) and re-scan (lower) curves obtained at a) 100 °C min^{-1} b) 50 °C min^{-1} c) 20 °C min^{-1} d) 10 °C min^{-1} and e) 2 °C min^{-1}.

2 °C min^{-1} (Fig. 2c, d and e) confirmed the prevalence of Form II in this sample compared with DMT W1 and that again it converted to Form I at the slower heating rates. The values of the enthalpies of fusion (see Tables 2 and 3 for comparison) confirmed the apparent higher ratio of Form II in sample W2. Estimates across the heating rates of the melting points of Form II and Form I in DMT W2 (Table 3) were 42.8 °C to 46.9 °C and 56.1 °C to 58.4 °C, values not dissimilar to those found for DMT W1 (Table 2).

The reheat curves for DMT W2 (Fig. 2) showed similar trends to DMT W1 except that the recrystallization exotherm was closer in position to the melting endotherm for Form II indicating that recrystallization to Form II in DMT W2 was not as easily accomplished as in DMT W1. This is evidenced by the lower enthalpies of fusion in the reheated sample of DMT W2 (Table 3) compared to those of DMT W1 (Table 2). The reasons for the increased difficulty in recrystallization to Form II are not easily understood since the initial heat should destroy the thermal history of the sample. In summary, both samples DMT W1 and W2 were a mixture of polymorphic forms whose melting points reflected the melting points found in the literature while explaining the literature discrepancies because two forms had not previously been identified. In addition, the T_g values (Tables 2 and 3) accounted for the potential for amorphicity in DMT because

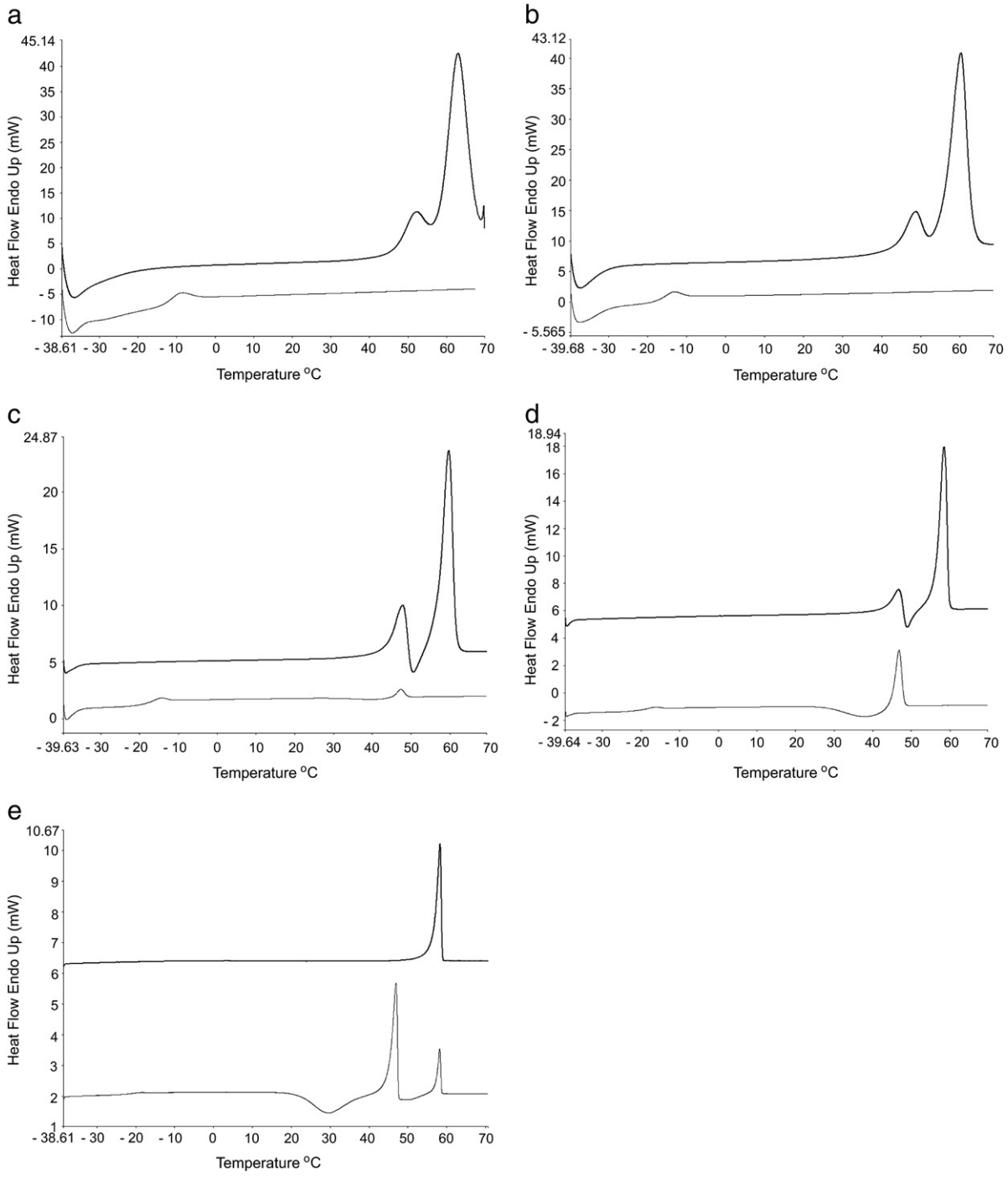

Fig. 4. DSC scans of sample Y2 showing initial scan (upper) and re-scan (lower) curves obtained at a) 100 °C min^{-1} b) 50 °C min^{-1} c) 20 °C min^{-1} d) 10 °C min^{-1} and e) 2 °C min^{-1}.

Table 2
Thermal data of DMT W1 obtained by DSC. [Key ($n = 3$) except where standard deviations are not given ($n = 1$), nt = no transition].

Heating rate	Initial heating				Secondary heating				
(°C min^{-1})	Form II		Form I			Form II		Form I	
	Onset (°C)	ΔH_f (J g^{-1})	Onset (°C)	ΔH_f (J g^{-1})	T_g (°C)	Onset (°C)	ΔH_f (J g^{-1})	Onset (°C)	ΔH_f (J g^{-1})
2	44.8 ± 0.1	10.0 ± 3.4	58.4 ± 0.1	91.9 ± 2.4	−21.8 ± 0.9	46.5 ± 0.1	98.3 ± 2.8	58.6	11.1
10	46.2 ± 0.1	26.1 ± 1.3	57.8 ± 0.1	86.8 ± 1.3	−19.2 ± 0.4	45.6 ± 0.1	51.8 ± 9.9	nt	nt
20	46.7 ± 0.1	23.0 ± 2.1	58.3 ± 0.1	85.2 ± 21.1	−18.5 ± 0.4	45.9 ± 0.1	12.1 ± 3.6	nt	nt
50	46.7 ± 0.3	42.5 ± 4.6	57.7 ± 0.1	57.9 ± 7.0	−16.7 ± 0.1	nt	nt	nt	nt
100	47.5	29.2	58.3	76.1	−13.0	nt	nt	nt	nt

Table 3
Thermal data of DMT W2 obtained by DSC. [Key ($n = 3$) except where standard deviations are not given ($n = 1$), nt = no transition].

Heating rate	Initial heating				Secondary heating				
(°C min^{-1})	Form II		Form I			Form II		Form I	
	Onset (°C)	ΔH_f (J g^{-1})	Onset (°C)	ΔH_f (J g^{-1})	T_g (°C)	Onset (°C)	ΔH_f (J g^{-1})	Onset (°C)	ΔH_f (J g^{-1})
2	42.8 ± 2.0	18.0 ± 6.0	57.3 ± 0.6	83.8 ± 0.7	−21.5	46.5 ± 0.1	98.3 ± 2.8	45.1	87.7
10	44.5 ± 0.3	43.8 ± 6.7	56.1 ± 0.4	64.1 ± 6.7	−20.0 ± 0.3	44.6 ± 0.0	10.9 ± 3.7	nt	nt
20	45.2 ± 0.4	58.4 ± 17.9	56.8 ± 0.4	42.1 ± 15.6	−18.5 ± 0.3	45.1 ± 0.2	0.9 ± 0.1	nt	nt
50	45.3 ± 0.2	73.5 ± 0.5	57.1 ± 0.3	0.5 ± 0.4	−16.3 ± 0.4	nt	nt	nt	nt
100	46.9	83.4	58.4	24.9	−12.8	nt	nt	nt	nt

Table 4
Thermal data of DMT Y1 obtained by DSC. [Key ($n = 1$), nt = no transition].

Heating rate	Initial heating				Secondary heating				
(°C min^{-1})	Form II		Form I			Form II		Form I	
	Onset (°C)	ΔH_f (J g^{-1})	Onset (°C)	ΔH_f (J g^{-1})	T_g (°C)	Onset (°C)	ΔH_f (J g^{-1})	Onset (°C)	ΔH_f (J g^{-1})
2	44.8	32.3	58.8	79.5	−20.8	45.6	92.1	nt	nt
10	44.9	29.9	56.9	79.7	−18.8	44.9	39.6	nt	nt
20	45.1	32.5	57.5	69.4	−17.8	45.4	12.1	nt	nt
50	45.0	22.8	56.4	38.4	−16.5	nt	nt	nt	nt
100	47.2	39.3	58.8	23.6	−12.0	nt	nt	nt	nt

Table 5
Thermal data of DMT Y1 obtained by DSC. [Key ($n = 1$), nt = no transition].

Heating rate	Initial heating				Secondary heating				
(°C min^{-1})	Form II		Form I			Form II		Form I	
	Onset (°C)	ΔH_f (J g^{-1})	Onset (°C)	ΔH_f (J g^{-1})	T_g (°C)	Onset (°C)	ΔH_f (J g^{-1})	Onset (°C)	ΔH_f (J g^{-1})
2	nt	nt	56.8	59.5	−20.6	45.0	92.7	57.1	21.7
10	43.8	15.8	56.5	69.8	−19.5	44.8	24.3	nt	nt
20	44.1	19.9	56.5	71.8	−17.5	45.2	2.1	nt	nt
50	44.3	7.1	55.6	50.4	−16.4	nt	nt	nt	nt
100	47.9	5.7	58.5	49.0	−12.4	nt	nt	nt	nt

of the closeness of the T_g to ambient temperatures. This also will explain the difficulty in obtaining a sample consisting of either pure Form I or pure Form II.

One attempt to obtain pure Form 1 was by heating the untreated samples to 45 °C and holding the samples at this temperature for 20 min to allow conversion of the Form II in the sample to Form I, prior to cooling and then re-scanning at 2 °C min^{-1}. Fig. 5 displays that this approach indeed worked and it was estimated that the heats of enthalpy for Form I obtained from DMT W1 and W2 were 93.4 and 86.8 J g^{-1}, respectively. Again there is the probability of amorphousness remaining in the sample following the isothermal hold.

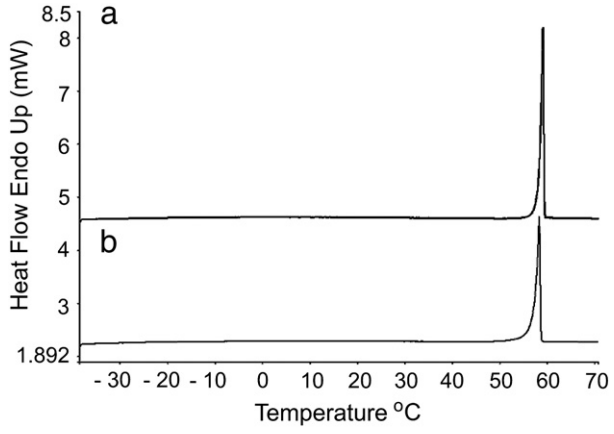

Fig. 5. DSC scans of samples W1 (a) and W2 (b) showing curves obtained at 2 °C min^{-1} after heat treatment at 45 °C.

Table 6
Summary of XRPD data for major peaks from DMT sample W1.[a]

Peak	2theta	FWHM	d-Value	Intensity	I/Io
1[b]	7.60	0.200	11.6223	793	70
2	9.04	0.212	9.7739	800	71
3	12.05	0.271	7.3384	402	36
4	12.86	0.259	6.8779	596	53
5	14.52	0.153	6.0951	254	23
6[b]	15.22	0.235	5.8163	1138	100
7	17.73	0.188	4.9982	723	64
8	18.17	0.259	4.8781	1023	90
9[b]	19.20	0.224	4.6187	690	61
10[b]	19.57	0.200	4.5322	489	43
11	19.90	0.176	4.4578	501	44
12	20.41	0.106	4.3475	320	29
13	20.54	0.235	4.3203	349	31
14	21.44	0.200	4.1409	254	23
15	22.35	0.271	3.9744	468	42
16	22.85	0.188	3.8885	486	43
17	23.19	0.259	3.8323	295	26
18	24.56	0.118	3.6215	263	24
19	25.42	0.224	3.5009	391	35
20	26.29	0.200	3.387	250	22
21	27.30	0.247	3.2639	481	43
22	30.65	0.376	2.9144	240	22

[a,b]: major peaks attributed to polymorphic Form II.

Table 7
Summary of XRPD data for major peaks from DMT sample W2.[a]

Peak no.	2theta	FWHM	d-Value	Intensity	I/Io
1[b]	7.56	0.141	11.6837	2827	60
2	8.96	0.176	9.861	567	12
3	11.97	0.153	7.3873	1002	22
4	12.77	0.153	6.9262	981	21
5[b]	15.17	0.153	5.8354	4737	100
6	17.68	0.106	5.0122	383	9
7	18.07	0.176	4.9049	811	18
8	18.17	0.059	4.8781	576	13
9[b]	19.75	0.071	4.4913	311	7
10	19.83	0.118	4.4734	319	7
11	22.29	0.118	3.9849	284	6
12	22.84	0.176	3.8902	483	11
13	24.09	0.200	3.6911	407	9
14	27.22	0.071	3.2733	302	7
15	30.68	0.129	2.9116	274	6

[a,b]: major peaks attributed to polymorphic Form II.

The two additional samples of DMT, crystallized from acetonitrile, were subjected to similar experimental conditions and studied. Macroscopically and microscopically, DMT Y1 and DMT Y2 were both yellow and appeared denser and less crystalline when using optical microscopy. DMT Y1 behaved similarly to DMT Y2 under DSC analysis conditions. Fig. 3a shows a preponderance of Form II in sample DMT Y1 as demonstrated for the heating rate of 100 °C min^{-1}. As the rates decreased the amount of unconverted Form II decreased (Fig. 3b–e). However the measured heats of fusion, with the exception of one sample, were consistently less for DMT Y1 (Table 4) than DMT W1 (Table 2) or DMT W2 (Table 3) and this confirmed the apparent increased amorphicity of this sample. Estimates across the heating rates (Table 4) of the melting points of Form II and Form I in DMT Y1 were 44.8 °C to 47.2 °C and 56.4 °C to 58.8 °C, respectively. The DSC re-scans of DMT Y1 (Fig. 3a–e) were similar to those of DMT W2 (Fig. 2a–e).

Table 8
Summary of XRPD data for major peaks from DMT sample Y1.[a]

Peak no.	2theta	FWHM	d-Value	Intensity	I/Io
1[b]	7.59	0.200	11.6376	1067	52
2	9.01	0.200	9.8064	1666	81
3	12.00	0.200	7.3689	1394	68
4	12.80	0.235	6.9100	1443	70
5	14.49	0.176	6.1077	241	12
6[b]	15.21	0.200	5.8201	1593	77
7	16.78	0.282	5.279	258	13
8	17.69	0.212	5.0094	795	39
9	18.10	0.235	4.8968	2078	100
10[b]	19.18	0.212	4.6235	1390	67
11[b]	19.55	0.200	4.5368	854	42
12	19.84	0.176	4.4711	683	33
13	20.45	0.212	4.3391	453	22
14	20.62	0.200	4.3037	373	18
15	21.43	0.235	4.1429	301	15
16	21.75	0.165	4.0826	276	14
17	22.31	0.247	3.9814	698	34
18	22.84	0.224	3.8902	419	21
19	23.14	0.188	3.8404	361	18
20	23.77	0.188	3.7400	294	15
21	24.14	0.247	3.6836	649	32
22	24.57	0.200	3.6201	262	13
23	25.38	0.247	3.5063	429	21
24	26.26	0.247	3.3908	325	16
25	26.63	0.165	3.3445	219	11
26	27.26	0.224	3.2686	827	40
27	27.81	0.176	3.2052	209	11
28	28.78	0.188	3.0994	266	13
29	30.60	0.341	2.9190	248	12
30	32.65	0.165	2.7403	212	11

[a,b]: major peaks attributed to polymorphic Form II.

Table 9
Summary of XRPD data for major peaks from DMT sample Y2.

Peak no.	2theta	FWHM	d-Value	Intensity	I/Io
1	9.02	0.200	9.7956	3418	32
2	12.02	0.200	7.3566	10,834	100
3	12.83	0.212	6.8940	8726	81
4	13.58	0.176	6.5149	325	3
5	15.03	0.212	5.8894	2277	22
6	17.71	0.188	5.0038	920	9
7	18.11	0.224	4.8942	5178	48
8	19.84	0.224	4.4711	887	9
9	20.52	0.165	4.3245	268	3
10	21.75	0.200	4.0826	449	5
11	22.30	0.212	3.9832	659	7
12	22.79	0.200	3.8986	427	4
13	23.82	0.153	3.7323	457	5
14	24.16	0.235	3.6805	4384	41
15	25.39	0.200	3.5050	600	6
16	25.72	0.235	3.4607	262	3
17	27.27	0.224	3.2675	1265	12
18	27.78	0.235	3.2086	269	3
19	28.79	0.259	3.0983	306	3
20	30.57	0.200	2.9218	289	3
21	32.65	0.271	2.7403	262	3
22	36.68	0.341	2.4479	261	3
23	41.11	0.282	2.1938	262	3

In comparison to the other three samples, DMT Y2 displayed an increased prevalence of Form I in the sample (Fig. 4a) at 100 °C min^{-1}. Indeed, at 2 °C min^{-1} there was little evidence for any melting or conversion from Form II to Form I (Table 5) during heating. The enthalpies of fusion (Table 5) of the initial heats were less than the other samples and confirmed that DMT Y2 initially was the most amorphous of the samples and contained the highest level of Form 1 of DMT. For DMT Y2 the melting ranges of Form II and Form I were 43.8 °C to 47.9 °C and 55.6 °C to 58.5 °C, respectively. The DSC re-scans (Fig. 4a–e) were once again similar to the other rescans with the exception of that obtained at 2 °C min^{-1} which displayed evidence for the melting of both Form II (seen in all other samples at 20°, 10° and 2 °C min^{-1}) and Form I which melted after some recrystallization. This

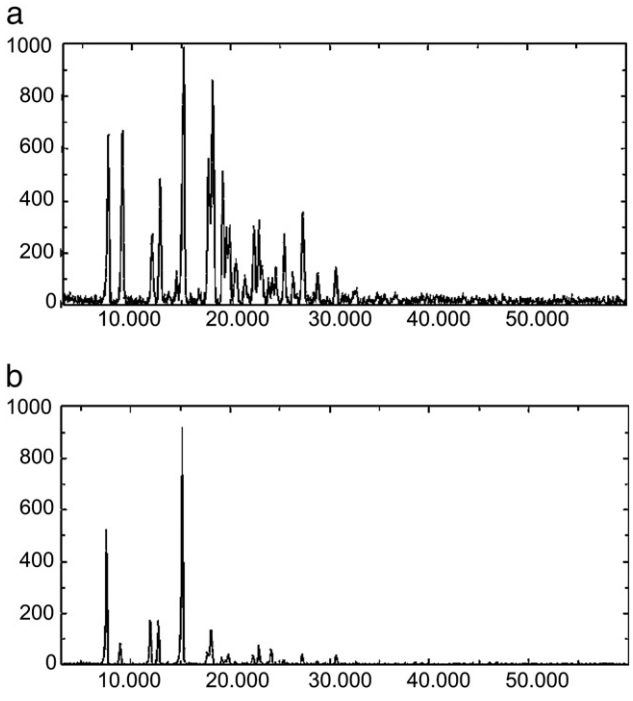

Fig. 6. XRPD patterns from DMT samples W1 (a) and W2 (b).

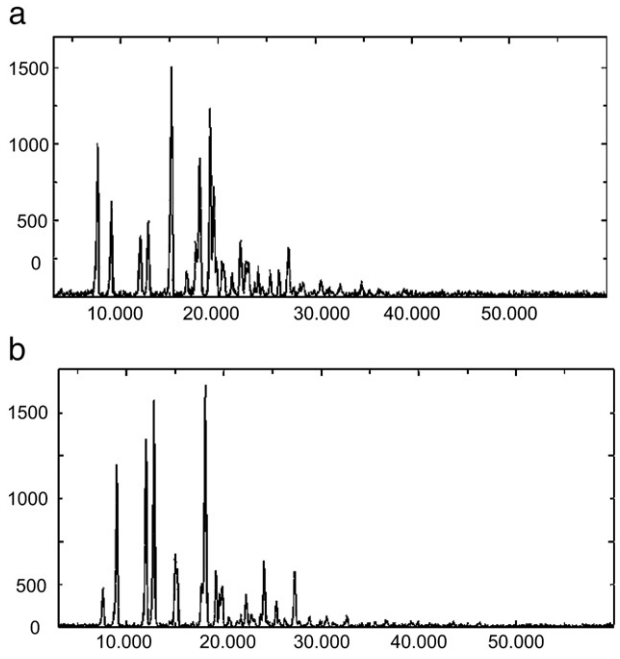

Fig. 7. XRPD patterns from DMT samples Y1 (a) and Y2 (b).

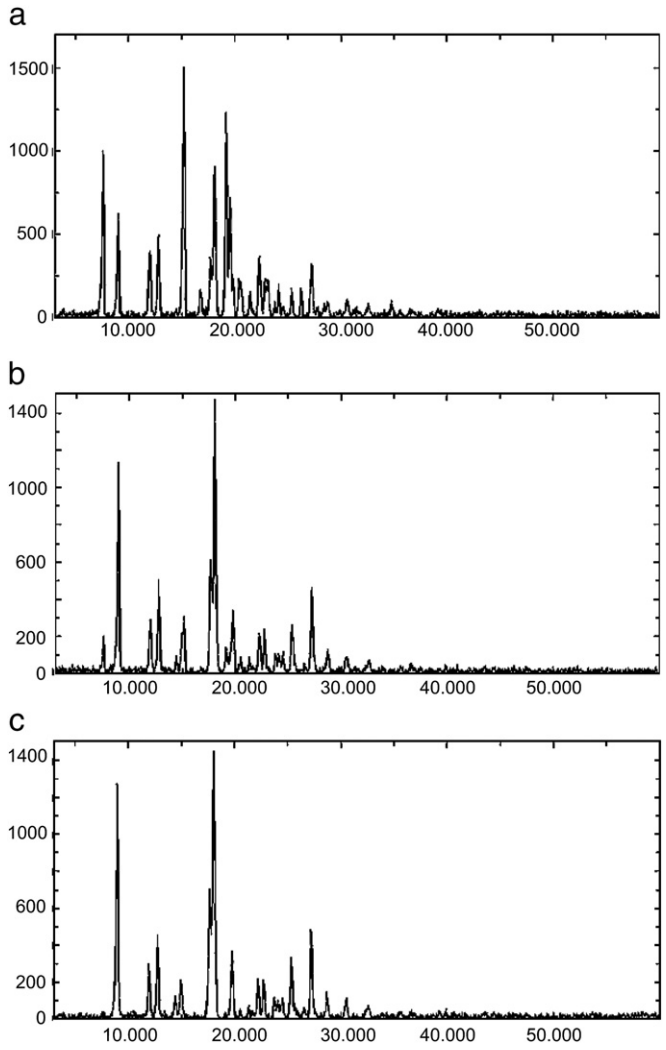

Fig. 8. XRPD patterns from DMT sample Y1 that were a) untreated b) lightly ground and c) more heavily ground.

probably equated to a conversion to Form I of ~18% given the value for the enthalpy of this event (21.7 J g^{-1}).

This raises interesting insight into the cause of yellowness in the two samples DMT Y1 and DMT Y2. There are the possibilities that the yellow color is caused either by the solvent used during recrystallization (hexane or acetonitrile) or by the presence of amorphousness in the sample. In an attempt to rule out solvent effects, and assuming that they were not lost from the enclosed DSC aluminum pans during heating, the effect of heating rate on the observed T_g values is shown in Tables 2 to 5. The apparent value of the T_g generally did increase with increase in heating rate, a phenomenon recognized for other glassy materials

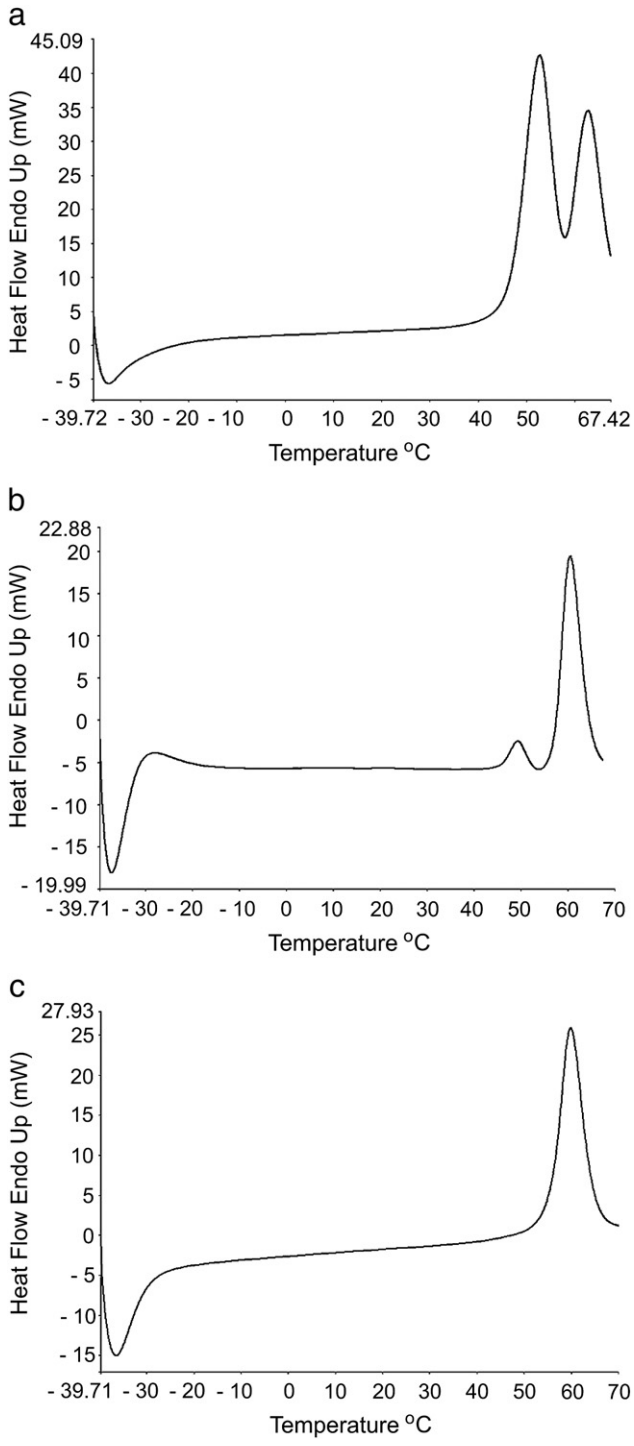

Fig. 9. DSC scans of sample Y1 from a) untreated b) lightly ground and c) more heavily ground material obtained at 100 °C min^{-1}.

[64] but the similarities in their values for the four samples at a given heating rate seemed to preclude the presence of a second impurity in the sample that promotes the color. The data thus suggest that this was solvent-mediated through increased amorphicity in the sample rather than a specific solvent–DMT interaction.

The XRPD data obtained from analysis of diffraction peaks from DMT samples W1, W2, Y1 and Y2 are provided in Tables 6–9, respectively. XRPD spectra obtained from DMT samples W1 and W2 are shown in Fig. 6, while those from DMT samples Y1 and Y2 are presented in Fig. 7. The XRPD pattern obtained from sample DMT Y2 exhibited fewer peaks than observed in DMT W1 and Y1 and this pattern was attributed to a predominance of the Form I polymorph. This was confirmed following XRPD analysis of heat treated samples held at 45 °C and determined to consist of Form I by DSC (Fig. 5). Peaks attributed to Form II were then identified and d-values assigned to prominent peaks characteristic of the two polymorphic forms determined in the mixed samples (Tables 6–9). The XRPD data from DMT W2 indicated that Form II was more prevalent in this sample while DMT W1 and Y1 presented as more equal mixtures of the polymorphs.

Sample preparations for XRPD analysis ideally include grinding of samples to decrease particle size and minimize preferential orientation of crystal lattices [26]. However, due to the low thermal stability of the Form II DMT polymorph, the incidental thermal energy introduced during mixing and grinding was found to alter the polymorph contents in the samples. This was verified by XRPD and fast scan DSC analysis (100 °C min^{-1}) of untreated samples and subsequent to light grinding and more heavily ground samples. A decrease in the content of the meta-stable Form II DMT polymorph was observed in all four DMT samples following grinding treatments; the extent of decrease was related to the degree of grinding. Typical XRPD and DSC spectra from grinding experiments are provided in Figs. 8 and 9 respectively, from analysis of sample DMT Y1 and demonstrate the reduction in Form II in lightly ground materials and the apparent absence of the meta-stable form following a heavier grind. Such data also confirm the apparent instability of the Form II of DMT.

4. Conclusion

The data provided in this paper have shown that DMT can be recrystallized from the solvents hexane and acetonitrile to give crystals that are a mixture of two polymorphs. The fact that two clearly exist explains the variation in melting points reported previously in the literature. It seems possible that use of the latter solvent gives crystals with a greater amorphousness and a yellow coloration. This solvent dependency was independent of the source of DMT, whether it was extracted from natural products or synthesized in the laboratory. The XRPD data correlated with the fast scan DSC data (Figs. 2–5a at 100 °C min^{-1}) and confirmed that all four samples studied contained at least two polymorphic forms of DMT with varying ratios of concentration, the proportion of which appears unrelated to sample color.

Acknowledgments

The authors wish to thank MCT/CNPq (process no. 620247/2008-8) and Pronex-FAPESB/CNPq (process no. 0015/2009) for financial support of this study. Dr. Timothy E. Mann (PETA Solutions) and Dr. Linda Seton (LJMU) are gratefully acknowledged for their helpful comments on the manuscript.

References

[1] A. Hoffer, H. Osmond, The Hallucinogens, Academic Press, Inc., Orlando, Florida, 1967.
[2] A.T. Shulgin, A. Shulgin, TIHKAL. The Continuation, Transform Press, Berkeley, 1997.
[3] R.J. Strassman, Human psychopharmacology of N, N-dimethyltryptamine, Behav. Brain Res. 73 (1996) 121–124.
[4] J. Riba, S. Romero, E. Grasa, E. Mena, I. Carrio, M.J. Barbanoj, Increased frontal and paralimbic activation following ayahuasca, the pan-amazonian inebriant, Psychopharmacology 186 (2006) 93–98.
[5] D. Fontanilla, M. Johannessen, A.R. Hajipour, N.V. Cozzi, M.B. Jackson, A.E. Ruoho, The hallucinogen N, N-dimethyltryptamine (DMT) is an endogenous sigma-1 receptor regulator, Science 323 (2009) 934–937.
[6] N.V. Cozzi, A. Gopalakrishnan, L.L. Anderson, J.T. Feih, A.T. Shulgin, P.F. Daley, A.E. Ruoho, Dimethyltryptamine and other hallucinogenic tryptamines exhibit substrate behavior at the serotonin uptake transporter and the vesicle monoamine transporter, J. Neural Transm. 116 (2009) 1591–1599.
[7] R.H.F. Manske, A synthesis of the methyltryptamine and some derivatives, Can. J. Res. 5 (1931) 592.
[8] S. Szára, Dimethyltryptamin: its metabolism in man; the relation of its psychotic effect to the serotonin metabolism, Experientia 12 (1956) 441–442.
[9] C.P.B. Martins, S. Freeman, J.F. Alder, T. Passie, S.D. Brandt, The profiling of psychoactive tryptamine drug synthesis focusing on mass spectrometry, Trends Anal. Chem. 29 (2010) 285–296.
[10] S.D. Brandt, C.P.B. Martins, Analytical methods for psychoactive N,N-dialkylated tryptamines, Trends Anal. Chem. 29 (2010) 858–869.
[11] D.J. McKenna, Clinical investigations of the therapeutic potential of ayahuasca: rationale and regulatory challenges, Pharmacol. Ther. 102 (2004) 111–129.
[12] A. Gaujac, S. Navickiene, M.I. Collins, S.D. Brandt, J.B. de Andrade, Analytical techniques for the determination of tryptamines and β-carbolines in plant matrices and in psychoactive beverages consumed during religious ceremonies and neo-shamanic urban practices, Drug Test. Anal. 4 (2012) 636–648.
[13] R.E. Schultes, A. Hofmann, The Botany and Chemistry of Hallucinogens, Charles C. Thomas, Springfield, 1980.
[14] S.A. Barker, E.H. McIlhenny, R. Strassman, A critical review of reports of endogenous psychedelic N,N-dimethyltryptamines in humans: 1955–2010, Drug Test. Anal. 4 (2012) 617–635.
[15] S.D. Brandt, S.A. Moore, S. Freeman, A.B. Kanu, Characterisation of the synthesis of N,N-dimethyltryptamine by reductive amination using gas chromatography ion trap mass spectrometry, Drug Test. Anal. 2 (2010) 330–338.
[16] C.P.B. Martins, M.A. Awan, S. Freeman, T. Herraiz, J.F. Alder, S.D. Brandt, Fingerprint analysis of thermolytic decarboxylation of tryptophan to tryptamine catalyzed by natural oils, J. Chromatogr. A 1210 (2008) 115–120.
[17] C.P.B. Martins, S. Freeman, J.F. Alder, S.D. Brandt, Characterisation of a proposed internet synthesis of *N*, *N*-dimethyltryptamine using liquid chromatography/electrospray ionisation tandem mass spectrometry, J. Chromatogr. A 1216 (2009) 6119–6123.
[18] S. Whitney, R. Grigg, A. Derrick, A. Keep, $[Cp^*IrCl_2]_2$-Catalyzed indirect functionalization of alcohols: novel strategies for the synthesis of substituted indoles, Org. Lett. 9 (2007) 3299–3302.
[19] M.S. Fish, N.M. Johnson, E.C. Horning, t-Amine oxide rearrangements. N,N-Dimethyltryptamine oxide, J. Am. Chem. Soc. 78 (1956) 3668–3671.
[20] D. Giron, Investigations of polymorphism and pseudo-polymorphism in pharmaceuticals by combined thermoanalytical techniques, J. Therm. Anal. Calorim. 64 (2001) 37–60.
[21] J.L. Ford, P. Timmins, Pharmaceutical thermal analysis: techniques and applications, Halsted Press, Chichester, 1989.
[22] D. Giron, Thermal analysis and calorimetric methods in the characterisation of polymorphs and solvates, Thermochim. Acta 248 (1995) 1–59.
[23] J.L. Ford, T.E. Mann, Fast-Scan DSC and its role in pharmaceutical physical form characterisation and selection, Adv. Drug Delivery Rev. 64 (2012) 422–430.
[24] C. McGregor, M.H. Saunders, G. Buckton, R.D. Saklatvala, The use of high-speed differential scanning calorimetry (Hyper-DSC™) to study the thermal properties of carbamazepine polymorphs, Thermochim. Acta 417 (2004) 231–237.
[25] J.A. Zeitler, D.A. Newnham, P.F. Taday, T.L. Threlfall, R.W. Lancaster, R.W. Berg, C.J. Strachan, M. Pepper, K.C. Gordon, T. Rades, Characterization of temperature-induced phase transitions in five polymorphic forms of sulfathiazole by terahertz pulsed spectroscopy and differential scanning calorimetry, J. Pharm. Sci. 95 (2006) 2486–2498.
[26] R. Jenkins, R.L. Snyder, Introduction to X-ray Powder Diffractometry, Wiley-Interscience, New York, 1996.
[27] L. Seton, D. Khamar, I.J. Bradshaw, G.A. Hutcheon, Solid state forms of theophylline: presenting a new anhydrous polymorph, Cryst. Growth Des. 10 (2010) 3879–3886.
[28] A. Gaujac, S.T. Martinez, A.A. Gomes, S.J. de Andrade, A. da Cunha Pinto, J.M. David, S. Navickiene, J.B. de Andrade, Application of analytical methods for the structural characterization and purity assessment of N, N-dimethyltryptamine, a potent psychedelic agent isolated from Mimosa tenuiflora inner barks, Microchem. J. 109 (2013) 78–83.
[29] O. Gonçalves de Lima, Observações sobre o "vinho da jurema" utilizado pelos índios Pancarú de Tacaratú (Pernambuco), Arq. Inst. Pesqui. Agron. Recife 4 (1946) 45–80.
[30] R.S.O. de Souza, U.P. Albuquerque, J.M. Monteiro, L.C. de Amorim, Jurema-Preta (*Mimosa tenuiflora* [Willd.] Poir.): a review of its traditional use, phytochemistry and pharmacology, Braz. Arch. Biol. Technol. 51 (2008) 931.
[31] J.S. Fitzgerald, A.A. Sioumis, Alkaloids of the Australian Leguminosae. V. The occurrence of methylated tryptamines in *Acacia maidenii* F. Muell, Aust. J. Chem. 18 (1965) 433–434.
[32] J.A. Grina, M.R. Ratcliff, F.R. Stermitz, Old and new alkaloids from *Zanthoxylum arborescens*, J. Org. Chem. 47 (1982) 2648–2651.
[33] B. Rovelli, G.N. Vaughan, Alkaloids of Acacia. I. N_bN_b-Dimethyltryptamine in *Acacia phlebophylla* F. Muell, Aust. J. Chem. 20 (1967) 1299–1300.
[34] J.A. Sintas, A.A. Vitale, Synthesis of ^{131}I derivatives of indolealkylamines for brain mapping, J. Label. Compd. Radiopharm. 39 (1997) 677–684.

[35] F.A. Hochstein, A.M. Paradies, Alkaloids of *Banisteria caapi* and *Prestonia amazonicum*, J. Am. Chem. Soc. 79 (1957) 5735–5736.
[36] M. Julia, J. Bagot, O. Siffert, Sur une nouvelle voie d'accès aux tryptamines, Bull. Soc. Chim. Fr. 4 (1973) 1424–1426.
[37] C.C.J. Culvenor, R. Dal Bon, L.W. Smith, Occurrence of indolealkylamine alkaloids in *Phalaris tuberosa* and *arundinacea*, Aust. J. Chem. 17 (1964) 1301–1304.
[38] M. Meckes-Lozoya, X. Lozoya, R.J. Marles, C. Soucy-Breau, A. Sen, J.T. Arnason, N,N-Dimethyltryptamine alkaloid in *Mimosa tenuiflora* bark (tepescohuite), Arch. Invest. Méd. (Méx) 21 (1990) 175–177.
[39] Wisconsin Alumni Research Foundation, A.E. Ruoho, A.R. Hajipour, U.B. Chu, D.A. Fontanilla, Sigma-1 Receptor Ligands and Methods of Use, WO2010059711 A1, 2010.
[40] E.S. Hall, F. McCapra, A.I. Scott, Biogenetic-type synthesis of the calycanthaceous alkaloids, Tetrahedron 23 (1967) 4131–4141.
[41] G. Häfelinger, M. Nimtz, V. Horstmann, T. Benz, Trifluoroacetylation of methylated derivatives of tryptamine and serotonin by different reagents. Synthesis, spectroscopic characterizations, and separations by capillary-gas-chromatography, Z. Naturforsch. B 54 (1999) 397–414.
[42] E. Wenkert, A.C. Kryger, Oxytryptamines, J. Indian Chem. Soc. 55 (1978) 1122–1124.
[43] I. Fleming, M. Woolias, A new synthesis of indoles particularly suitable for the synthesis of tryptamines and tryptamine itself, J. Chem. Soc., Perkin Trans. 1 (3) (1979) 829–837.
[44] S. Ghosal, B. Mukherjee, Alkaloids of *Desmodium pulchellum* Benth. ex Baker, Chem. Ind. (1964) 1800.
[45] R.V. Heinzelman, J. Szmuszkovicz, Recent studies in the field of indole compounds, Prog. Drug Res. 6 (1963) 75–150.
[46] A. Ueno, Y. Ikeya, S. Fukushima, T. Noro, K. Morinaga, H. Kuwano, Studies on the constituents of *Desmodium caudatum* DC, Chem. Pharm. Bull. 26 (1978) 2411–2416.
[47] K. Bodendorf, A. Walk, Darstellung und Reduktion von Indolyl-(3)-aminomethyl-ketonen, Arch. Pharm. 294 (1961) 484–487.
[48] I.J. Pachter, D.E. Zacharias, O. Ribeiro, Indole alkaloids of *Acer saccharinum* (the Silver Maple), *Dictyoloma incanescens*, *Piptadenia colubrina*, and *Mimosa hostilis*, J. Org. Chem. 24 (1959) 1285–1287.
[49] H.G. Boit, Ergebnisse der Alkaloid-Chemie bis 1960 unter Berücksichtigung der Fortschritte seit 1950, Akademie-Verlag, Berlin, 1961.
[50] H. Morimoto, N. Matsumoto, Über Alkaloide, VI. Inhaltsstoffe von *Lespedeza bicolor* var. *japonica*, II, Justus Liebigs Ann. Chem. 692 (1966) 194–199.
[51] H. Morimoto, H. Oshio, Über Alkaloide, V. Inhaltsstoffe von *Lespedeza bicolor* var. *japonica*, I. Über Lespedamin, ein neues Alkaloid, Justus Liebigs Ann. Chem. 682 (1965) 212–218.
[52] A.T. Shulgin, Profiles of psychedelic drugs: DMT, J. Psychedelic Drugs 8 (1976) 167–168.
[53] T. Hoshino, K. Shimodaira, Synthese des Bufotenins und über 3-Methyl-3-β-oxyäthyl-indolenin. Synthesen in der Indol-Gruppe. XIV, Justus Liebigs Ann. Chem. 520 (1935) 19–30.
[54] H.R. Arthur, S.N. Loo, J.A. Lamberton, N_b-Methylated tryptamines and other constituents of *Acacia confusa* Merr. of Hong Kong, Aust. J. Chem. 20 (1967) 811–813.
[55] J. Poisson, Note sur le "Natem", boisson toxique péruvienne et ses alcaloïdes, Ann. Pharm. Fr. 23 (1965) 241–244.
[56] C. Kan-Fan, B.C. Das, P. Boiteau, P. Potier, Alcaloïdes de *Vepris ampody* (Rutacées), Phytochemistry 9 (1970) 1283–1291.
[57] R. Bergin, D. Carlström, G. Falkenberg, H. Ringertz, Preliminary X-ray crystallographic study of some psychoactive indole bases, Acta Cryst. B. 24 (1968) 882.
[58] S. Moura, F.G. Carvalho, C.D. Rodrigues de Oliveira, E. Pinto, M. Yonamine, qNMR: an applicable method for the determination of dimethyltryptamine in ayahuasca, a psychoactive plant preparation, Phytochem. Lett. 3 (2010) 79–83.
[59] G. Falkenberg, The crystal and molecular structure of (N, N)-dimethyltryptamine, Acta Cryst. B 28 (1972) 3075–3083.
[60] J.C. Van Miltenburg, M.A. Cuevas-Diarte, The influence of sample mass, heating rate and heat transfer coefficient on the form of DSC curves, Thermochim. Acta 156 (1989) 291–297.
[61] O. Bley, J. Siepmann, R. Bodmeier, Importance of glassy-to-rubbery state transitions in moisture-protective polymer coatings, Eur. J. Pharm. Biopharm. 73 (2009) 146–153.
[62] T. Threlfall, Structural and thermodynamic explanations of Ostwald's rule, Org. Process. Res. Dev. 7 (2003) 1017–1027.
[63] M.M. Parmar, O. Khan, L. Seton, J.L. Ford, Polymorph selection with morphology control using solvents, Cryst. Growth Des. 7 (2007) 1635–1642.
[64] G. Buckton, A.A. Adeniyi, M. Saunders, A. Ambarkhane, HyperDSC studies of amorphous polyvinylpyrrolidone in a model wet granulation system, Int. J. Pharm. 312 (2006) 61–65.